Electronic Supplementary Material (ESI) for Nanoscale

Supplementary Materials

Intrinsic Region Length Scaling of Heavily Doped Carbon Nanotube *p-i-n* Junctions

Zheng Li,[1] Jiaxin Zheng,[1,2] Zeyuan Ni,[1] Ruge Quhe,[1,2] Yangyang Wang,[1] Zhengxiang Gao,[1] and Jing Lu[1,*]

[1] State Key Laboratory of Mesoscopic Physics and Department of Physics, Peking University, Beijing 100871, P. R. China

[2] Academy for Advanced Interdisciplinary Studies, Peking University, Beijing 100871, P. R. China

[*]Corresponding author: jinglu@pku.edu.cn

1. Semi-logarithm fitting plots of the forward peak current and the current under -1.0 V bias of our SWCNT *p-i-n* junctions versus the intrinsic region length

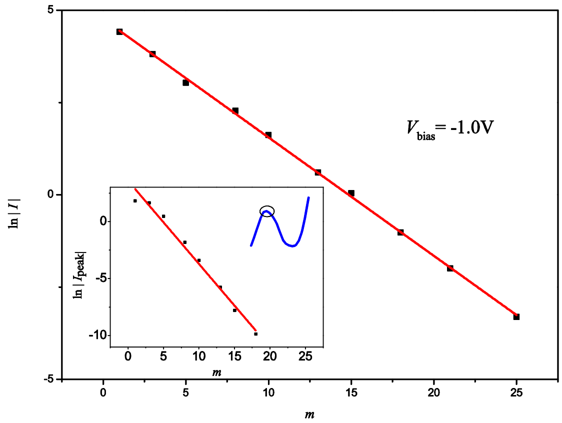

Figure S1. The semi-logarithm fitting plots of the current under V_{bias} = -1.0 V (main panel) and the forward peak current (inset) of our SWCNT *p-i-n* junctions versus the repetition number *m*. The black dots indicate the raw data. The red lines indicate the linear fitting results. Fairly good linear correlations can be observed in both cases.

2. The derivation of Eq (3)

Under WKB approximation, using Fowler-Nordheim formula, we have the transmission probability (TP) of a triangular potential barrier as

$$\mathrm{TP} = exp\,(-\frac{8\pi}{3}\frac{\sqrt{2em}}{h}\varphi^{1/2}D) \tag{S1}$$

where *e* and m are the charge and mass of electrons, *h* the Plank constant, φ the barrier height, and *D* the barrier width.

In part 1, we roughly consider the barrier in the intrinsic region as triangular, and we can get

$$\mathrm{TP'} = \exp\,(-\frac{8\pi}{3}\frac{\sqrt{2em}}{h}\frac{E_g^{3/2}}{\Delta}L) \tag{S2}$$

where Δ is the energy difference between the bottoms of the conduction bands of the *p* and *n* regions, *L* the intrinsic region length, and E_g the band gap (Figure S2). The current can be calculated as

$$I = C \times \int \mathrm{TP'} \times \mathrm{DOS}(p \text{ region}) \times \mathrm{DOS}(n \text{ region}) \times f_p(E-\mu_p) \times f_n(E-\mu_n) \times \mathrm{d}E$$

(S3)

where C is a constant, E the energy of the interband tunneling electrons, DOS(p/n region) the density of states in the p/n region, $f_{p/n}(E)$ the Fermi-Dirac distribution function for the p/n region, and $\mu_{p/n}$ the electrochemical potential of the p/n region. DOS and $f_{L/R}$ are related to V_{bias} but independent of L, and TP' is independent of E. Therefore, Eq. S3 can be written as

$$I = C \times \mathrm{TP'} \times \mathrm{Int}(V_{\mathrm{bias}}) \tag{S4}$$

where $\mathrm{Int}(V_{\mathrm{bias}})$ is the integral in Eq. S3 without TP'. We can further get |RR| in part 1 as

$$|\mathrm{RR}| = \left|\frac{I_-}{I_+}\right| = \left|\frac{\mathrm{Int}(-V_{\mathrm{bias}})}{\mathrm{Int}(V_{\mathrm{bias}})}\right| \times \frac{\mathrm{TP'}_-}{\mathrm{TP'}_+} = A \times \exp\left[-\frac{8\pi}{3}\frac{\sqrt{2em}}{h}E_g^{3/2}\left(\frac{1}{\Delta_-}-\frac{1}{\Delta_+}\right)L\right] = A \times \exp(B \times L) \tag{S5}$$

where $\mathrm{TP'}_{+/-}$ and $\Delta_{+/-}$ is TP' and Δ under forward/reverse bias, respectively, and we have $\Delta_+ < \Delta_-$. Therefore, $A = \left|\mathrm{Int}(-V_{\mathrm{bias}})/\mathrm{Int}(V_{\mathrm{bias}})\right|$ and $B = -\frac{8\pi}{3}\frac{\sqrt{2em}}{h}E_g^{3/2}\left(\frac{1}{\Delta_-}-\frac{1}{\Delta_+}\right)$ are both positive and independent of L.

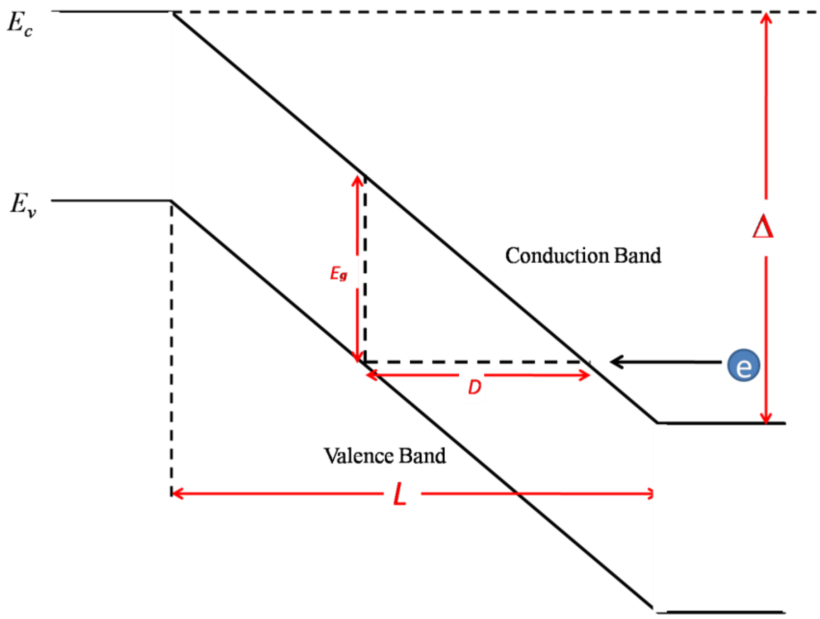

Figure S2. The simplified band diagram of the *p*-*i*-*n* junctions. We assume that the band shape of the intrinsic region is linear. Under such an approximation, all interband tunneling electrons face barriers of the same height and width under a fixed bias. Therefore, the transmission probability is independent from the energy of electrons.

3. A comparison of the I-V_{bias} curves of the SWCNT *p-i-n* junction with m = 1 based on DFT and the semi-empirical model

We present a comparison of the I-V_{bias} curves of the SWCNT *p*-*i*-*n* junction with m = 1 based on DFT and the semi-empirical model in the following figure. We can see the main properties of these two curves are similar: they both have obvious NDR effects, and the ranges of the NDR regions are similar. (0.3 V for the semi-empirical model and 0.2 V for the DFT model). Therefore, the semi-empirical model is reliable.

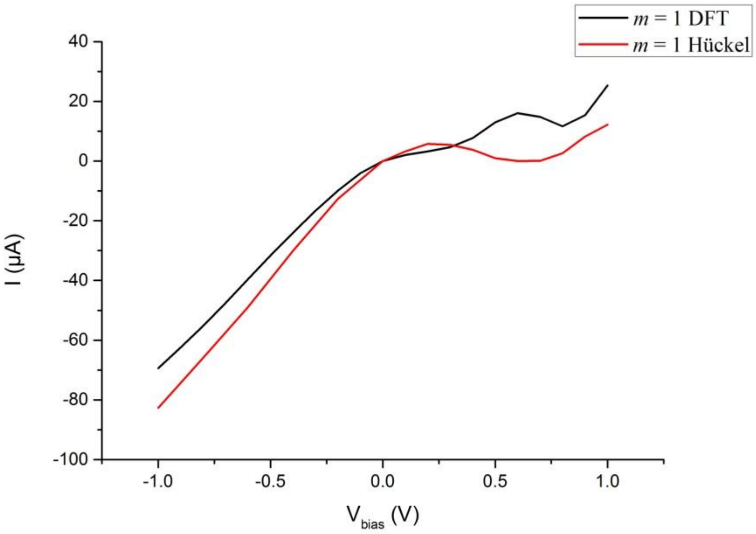

Figure S3. A comparison of the I-V_{bias} curves of the SWCNT *p*-*i*-*n* junction with m = 1 based on DFT and the semi-empirical model. The red line and the black line indicate the results based on DFT and the extended Hückel model, respectively.

4. The mechanism of the observed NDR effect based on the band structure

The mechanism of the observed NDR in the SWCNT *p*-*i*-*n* junction is the same as that of Esaki diodes. We present the band diagrams of our *p*-*i*-*n* junction as follows. The electrodes are heavily doped, so the Fermi level induces into the valence band of the left electrode (*p* region) and the conduction band of the right electrode (*n* region) (Figure S4 (a)). Therefore, applied a relatively small positive bias, electrons from the conduction band of the *n* region start to tunnel into the valence band of the *p* region (Figure S4 (b)). Enhancing the bias voltage, the overlap region of density of states (DOS) in the *n* and *p* region reaches a maximum value, and thus the current reaches a peak (Figure S4 (c)). Further enhancing the bias suppresses the interband tunneling because the available DOS in the *p* region decreases since the Fermi level in the *n* region induces into the band gap of the *p* region (Figure S4 (d)). When there is no available DOS in the *p* region for electrons of the *n* region, the tunneling current is very small and the electron injection current (thermionic current) starts to dominate the transport (Figure S4 (e)). Applied a negative bias, there is always available

DOS in the n region for electrons in the p region, and thus the overlap region increases monotonically with the bias voltage (Figure S4 (f)). Therefore, the reverse current grows up monotonically with the bias.

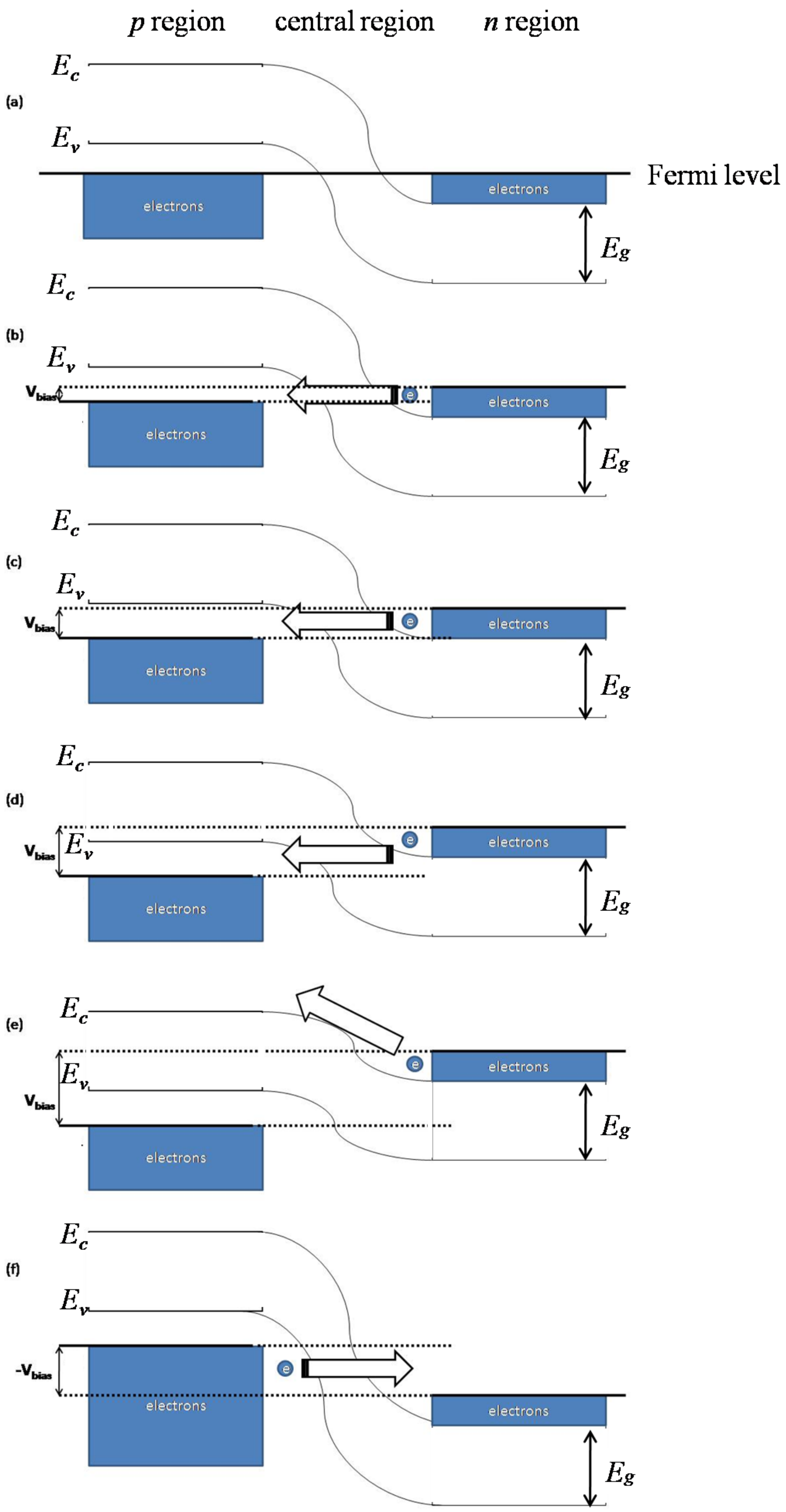

Figure S4. The band diagrams of our *p*-*i*-*n* junctions (a) under zero bias, (b) under a reletively small positive bias and the current starts to increase, (c) the current reaches a peak under positive bias, (d) the current decreses under positive bias, (e) under a relatively large positive bias and the electron injection current dominates the transport, and (f) under negative bias. The arrow with black bottom stands for the interband tunneling current and the arrow without black bottom stands for the electron injection current (thermionic current).

5. The transmission spectra and the PDOSs of the SWCNT *p-i-n* junction with *m* = 8

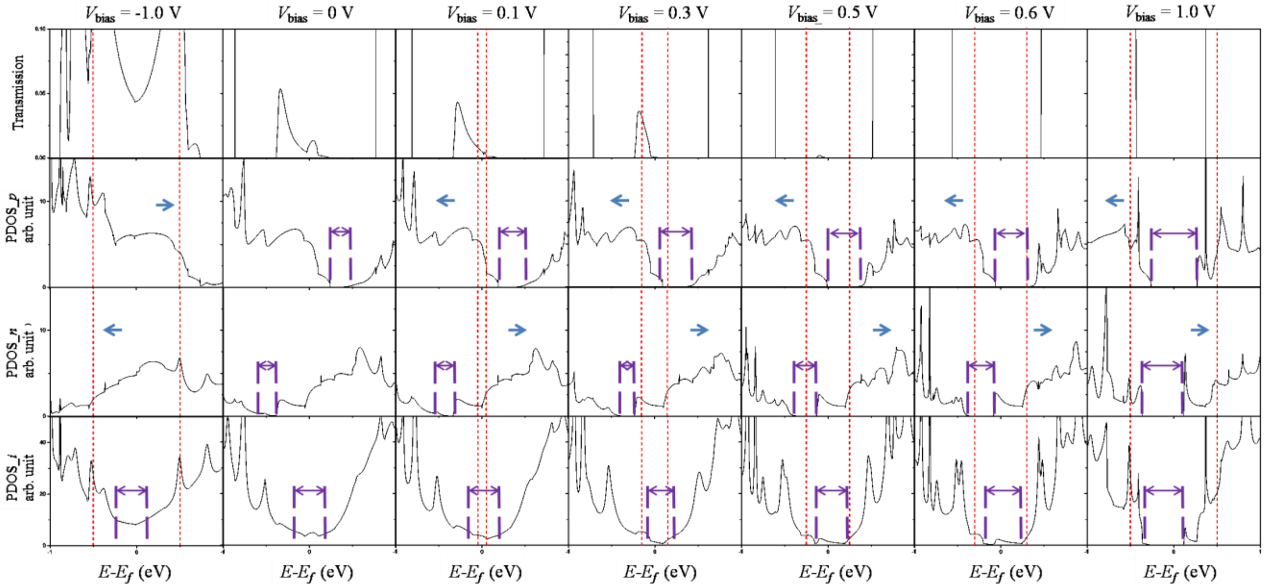

Figure S5: The transmission spectra and the PDOSs of the *p* region (PDOS_*p*), *n* region (PDOS_*n*) and intrinsic region (PDOS_*i*) of the SWCNT *p*-*i*-*n* junction with *m* = 8 under V_{bias} = -1.0, 0.1, 0.3, 0.5, 0.6, and 1.0 V. The red dash lines indicate the bias window. The blue arrows indicate the moving direction of the PODSs. The purple arrows and dash lines indicate the pseudo gaps of the PDOSs.